genes

MDPI

*Article*

# Mapping Inherited Genetic Variation with Opposite Effects on Autoimmune Disease and Four Cancer Types Identifies Candidate Drug Targets Associated with the Anti-Tumor Immune Response

**Junyu Chen [1], Michael P. Epstein [2], Joellen M. Schildkraut [1] and Siddhartha P. Kar [3,4,5,*]**

[1] Department of Epidemiology, Rollins School of Public Health, Emory University, Atlanta, GA 30322, USA; junyu.chen@emory.edu (J.C.); joellen.m.schildkraut@emory.edu (J.M.S.)
[2] Department of Human Genetics, School of Medicine, Emory University, Atlanta, GA 30322, USA; mpepste@emory.edu
[3] Early Cancer Institute, University of Cambridge, Cambridge CB2 0AH, UK
[4] Centre for Cancer Genetic Epidemiology, University of Cambridge, Cambridge CB1 8RN, UK
[5] Department of Oncology, University of Cambridge, Cambridge CB2 0AH, UK
* Correspondence: sk718@cam.ac.uk

**Abstract: Background**: Germline alleles near genes encoding certain immune checkpoints (*CTLA4*, *CD200*) are associated with autoimmune/autoinflammatory disease and cancer, but in opposite ways. This motivates a systematic search for additional germline alleles with this pattern with the aim of identifying potential cancer immunotherapeutic targets using human genetics. **Methods**: Pairwise fixed effect cross-disorder meta-analyses combining genome-wide association studies (GWAS) for breast, prostate, ovarian and endometrial cancers (240,540 cases/317,000 controls) and seven autoimmune/autoinflammatory diseases (112,631 cases/895,386 controls) coupled with in silico follow-up. **Results**: Meta-analyses followed by linkage disequilibrium clumping identified 312 unique, independent lead variants with $p < 5 \times 10^{-8}$ associated with at least one of the cancer types at $p < 10^{-3}$ and one of the autoimmune/autoinflammatory diseases at $p < 10^{-3}$. At each lead variant, the allele that conferred autoimmune/autoinflammatory disease risk was protective for cancer. Mapping led variants to nearest genes as putative functional targets and focusing on immune-related genes implicated 32 genes. Tumor bulk RNA-Seq data highlighted that the tumor expression of 5/32 genes (*IRF1*, *IKZF1*, *SPI1*, *SH2B3*, *LAT*) was each strongly correlated (Spearman's $\rho > 0.5$) with at least one intra-tumor T/myeloid cell infiltration marker (*CD4*, *CD8A*, *CD11B*, *CD45*) in every one of the cancer types. Tumor single-cell RNA-Seq data from all cancer types showed that the five genes were more likely to be expressed in intra-tumor immune versus malignant cells. The five lead SNPs corresponding to these genes were linked to them via the expression of quantitative trait locus mechanisms and at least one additional line of functional evidence. Proteins encoded by the genes were predicted to be druggable. **Conclusions**: We provide population-scale germline genetic and functional genomic evidence to support further evaluation of the proteins encoded by *IRF1*, *IKZF1*, *SPI1*, *SH2B3* and *LAT* as possible targets for cancer immunotherapy.

**Keywords:** autoimmune disease; cancer; autoinflammatory disease; genome-wide association study; breast cancer; ovarian cancer; endometrial cancer; prostate cancer



Academic Editor: Jing Yang

Received: 18 April 2025
Revised: 11 May 2025
Accepted: 13 May 2025
Published: 14 May 2025

**Citation:** Chen, J.; Epstein, M.P.; Schildkraut, J.M.; Kar, S.P. Mapping Inherited Genetic Variation with Opposite Effects on Autoimmune Disease and Four Cancer Types Identifies Candidate Drug Targets Associated with the Anti-Tumor Immune Response. *Genes* **2025**, *16*, 575. https://doi.org/10.3390/genes16050575

## 1. Introduction

Immunotherapy of cancer through inhibition of the immune checkpoints CTLA-4 and PD-1/PD-L1 has led to dramatic improvements in survival for patients who respond to these treatments across several cancer types. An emerging body of evidence suggests that inherited or germline genetic variation with established association with autoimmune disease susceptibility, when aggregated into multi-variant polygenic scores predictive of autoimmune disease, is associated with the risk of developing immune-related adverse events in cancer patients receiving immune checkpoint inhibitors and, in turn, with better therapeutic response and survival likely due to the enhanced autoimmune anti-tumor activity [1,2]. Germline single nucleotide polymorphisms (SNPs) known to be associated with autoimmune disease risk have also been shown to associate with intra-tumor immune cell infiltrate levels underscoring the importance of the germline genome in regulating the anti-tumor immune response [3,4].

A SNP rs231779, associated at genome-wide significance ($p < 5 \times 10^{-8}$) with rheumatoid arthritis, hypothyroidism and type 1 diabetes risk, was recently found to be associated with predisposition to melanoma and keratinocyte cancers [5]. There are three notable features of this finding: the gene nearest to rs231779 is *CTLA4*, the allele of rs231779 that increases autoimmune disease risk is protective for melanoma and keratinocyte cancers and rs231779, while being associated with melanoma risk ($p = 3.6 \times 10^{-4}$), did not reach the conventional genome-wide significance threshold ($p < 5 \times 10^{-8}$). Even more recently, germline alleles near genes encoding the CD200 immune checkpoint—specifically, *CD200*, *CD200R1* that encodes the receptor for CD200, and *DOK2* that encodes a downstream adapter protein—were found to have significant associations with, but opposite effects on, autoimmune hypothyroidism, asthma and eczema versus basal cell carcinoma risks, recapitulating the pattern of pleiotropy observed at the *CTLA4* genomic locus [6]. Moreover, tumor *CD200R1* expression was strongly correlated (Spearman's $\rho > 0.5$) with the expression of at least one of four commonly used T cell and myeloid infiltration markers (*CD4*, *CD8A*, *CD11B* and *CD45*) in tumors from multiple cancer types in The Cancer Genome Atlas (TCGA; [6]). These observations have formed the basis for the development of an anti-CD200R1 antibody as a CD200 checkpoint inhibitor with a promising pre-clinical profile that is now in Phase 1/2a trials [6].

A vast amount of genome-wide association study (GWAS) data for both autoimmune/autoinflammatory conditions and cancers of the breast, prostate, ovary and endometrium now exist in the public domain. These four cancer types are typically considered immune "cold". Immune cold tumors are tumors that generally lack substantial T cell infiltration or contain greater numbers of immunosuppressive cells and therefore they usually do not trigger strong immune responses and are harder to treat using currently available immunotherapy [7]. However, despite the striking pleiotropic pattern of opposite but significant allelic effects exhibited by SNPs near well-established (CTLA-4) and novel (CD200R1) immune-oncology targets, there is no published catalog of SNPs that demonstrate this pattern from systematic mining of GWAS data for breast, prostate, ovarian and endometrial cancers. To address this gap and identify potential additional candidates for follow up in immunotherapeutic drug development programs, here we present the results from large-scale pairwise cross-disorder meta-analyses combining GWAS data on 112,631 autoimmune/autoinflammatory disease and 240,540 breast, prostate, ovarian and endometrial cancer cases. Our analyses focused on these four cancer types and seven adult autoimmune/autoinflammatory diseases—type 1 diabetes (T1D), rheumatoid arthritis (RA), Hashimoto's thyroiditis (HT), multiple sclerosis (MS), systemic lupus erythematosus (SLE), ulcerative colitis (UC) and Crohn's disease (CD). We sought to identify independent (in terms of linkage disequilibrium), genome-wide significant lead SNPs in each

pairwise meta-analysis where the same allele was nominally associated with an autoimmune/autoinflammatory disease and a cancer type but with the opposite direction of effect and adapted our meta-analytic approach to power the discovery of such SNPs. We mapped each identified lead SNP to its nearest gene as its most likely regulatory target and focused on the nearest genes with known immune system function. We then found five genes among the 32 immune-related nearest genes whose tumor expression was strongly correlated with the tumor expression of at least one T cell or myeloid infiltration marker in all four cancer types (2696 breast, prostate, ovarian and endometrial tumors). Each of the five genes was, in general, more highly expressed in tumor-infiltrating immune cells versus malignant cells across 29 single-cell RNA sequencing data sets obtained from these four cancer types. We confirmed that the lead SNPs corresponding to the five genes—*IRF1*, *IKZF1*, *SPI1*, *SH2B3* and *LAT*—were expression quantitative trait loci for these genes, allowing us to establish the directionality of the relationship between their expression and cancer risk and infer the direction of pharmacological modulation required. We also identified additional functional genomic evidence to consolidate the link between these lead SNPs and the five corresponding genes and determined that the proteins encoded by the genes were potentially "druggable" via antibodies or proteolysis targeting chimeras (PROTACs).

## 2. Materials and Methods

### 2.1. GWAS Data Sets

We used publicly available GWAS summary statistics for four cancer types and seven autoimmune/autoinflammatory diseases in our study of pleiotropic SNPs across these cancers and autoimmune diseases (Supplementary Table S1). Summary statistics consisted of SNP rs number/identifier, chromosome, position, effect allele, other allele, effect allele frequency, imputation quality score, effect size estimate or β coefficient from regression models for genetic association, standard error for this estimate and *p*-value. All summary statistics were based on GWAS conducted in individuals of European or predominantly European ancestry and the human genome build for these data was GRCh37. SNPs with minor allele frequency < 0.5% and imputation quality score ($r^2$) < 0.3 were excluded, except for the GWAS of CD and UC, which did not report allele frequency and imputation quality metrics in the publicly available data sets.

Breast cancer risk GWAS summary statistics were obtained from meta-analyses of 122,977 overall, 69,501 estrogen receptor (ER)-positive and 21,468 ER-negative breast cancer cases, with each set of cases compared against 105,974 controls [8]. GWAS summary statistics for ovarian cancer risk were obtained from a meta-analysis involving 25,509 cases (that included 13,037 high-grade serous cases) and 40,941 controls [9]. GWAS summary statistics were obtained from a meta-analysis of 79,148 cases and 61,106 controls for prostate cancer risk [10]; and from a meta-analysis involving 12,906 cases and 108,979 controls for endometrial cancer risk [11].

CD GWAS summary statistics were sourced from a meta-analysis of 4474 cases and 9500 controls [12]. The same study also reported UC GWAS summary statistics from a meta-analysis involving 4173 cases and 9500 controls [12]. Summary statistics were obtained from GWAS meta-analyses of 29,880 cases and 73,758 controls for RA [13], 7219 cases and 15,991 controls for SLE [14], 30,234 cases and 725,172 controls for HT [15], 14,498 cases and 24,091 controls for MS [16] and 22,153 cases and 37,374 controls for T1D [17].

### 2.2. Meta-Analysis for Each Autoimmune/Autoinflammatory Disease and Cancer Pair

We first performed a meta-analysis of each autoimmune/autoinflammatory disease-cancer type or subtype pair using the fixed effect inverse-variance weighted method implemented in METAL [18]. Apart from analyzing overall breast, prostate, ovarian and

endometrial cancer GWAS we also separately evaluated ER-positive and -negative breast and high-grade serous ovarian cancers since these subtypes had substantial GWAS sample sizes in their own right and are known to have distinct genetic architectures. Thus, we effectively crossed seven autoimmune/autoinflammatory diseases GWAS with seven cancer type/subtype GWAS in the paired meta-analyses. We only included SNPs with $p < 10^{-3}$ for association with both cancer and autoimmune disease in each pairwise meta-analysis, with the choice of this $p < 10^{-3}$ threshold guided by our previously published cross-cancer GWAS meta-analysis [19]. In order to obtain meta-analysis results such that SNPs that have opposite effects on the two outcomes (autoimmune/autoinflammatory disease versus cancer type/subtype) would be identified at combined genome-wide significance ($p < 5 \times 10^{-8}$) under the fixed effect model, β coefficients (effect size estimates) from GWAS summary statistics for all the autoimmune diseases were multiplied by $-1$ before the meta-analysis thus reversing the sign on the estimate while keeping the effect allele the same. In addition, after reversing the sign and performing each pairwise meta-analysis, Cochrane's Q test for heterogeneity was applied and SNPs with $p < 0.05$ for heterogeneity were excluded from further analysis.

Meta-analysis results from METAL were used as input for the Functional Mapping and Annotation (FUMA) platform to identify lead SNPs associated with both a cancer and an autoimmune/autoinflammatory disease [20] using linkage disequilibrium (LD) clumping. For LD clumping in FUMA, the maximum (largest numeric value) *p*-value of lead SNPs was set as $5 \times 10^{-8}$; the maximum distance between LD blocks to merge into a single region was set to 1 Mb; and the LD $r^2$ threshold to define lead SNPs was set to 0.1. The combination of the sign reversal process described above, the application of the heterogeneity test and the $p < 10^{-3}$ individual trait and $p < 5 \times 10^{-8}$ cross-trait meta-analysis thresholds collectively ensured that our final set of lead SNPs were (1) nominally associated with at least one autoimmune/autoinflammatory disease and one cancer type/subtype, (2) the direction of allelic effect was opposite between the autoimmune/autoinflammatory disease and cancer, (3) the allelic effect size was otherwise homogeneous across the traits and (4) the combined cross-trait association was genome-wide significant.

### *2.3. Identification of Immune-Related Genes Among Genes Nearest to Lead SNPs*

Large-scale systematic evaluation of the GWAS literature has suggested that in about 70% of the instances, the gene nearest to a GWAS-identified lead SNP was the most likely target gene of that lead SNP locus [21]. Therefore, we used the FUMA pipeline version 1.6.1 to annotate the lead SNPs identified in each pairwise cancer-autoimmune/autoinflammatory disease meta-analysis with its nearest gene. We hypothesized that some, but not necessarily all, of these genes would have functions related to the immune system and to identify this subset of immune-related genes we merged our nearest gene list with a list of 1793 immune-related genes curated by the ImmPort project [22,23] to select the genes that were in common to both lists. Second, as a strategy to identify additional immune-related genes potentially missed by the ImmPort approach we performed pathway enrichment analysis for the combined list of all nearest genes identified across all the pairwise meta-analyses. We used the Enrichr platform [24] for the pathway analysis, applying the hypergeometric test to identify pathway overrepresentation and four pathway databases to obtain pathway annotations (Reactome 2022, WikiPathway 2021, KEGG 2021 and MSigDB Hallmark 2020). We then assessed the top 10 results from each pathway database, selected the immune-related pathways among the top 10 and picked the nearest genes from our list that were driving that immune-related pathway association as per Enrichr.

### 2.4. Tumor Bulk and Single-Cell RNA-Seq Analyses to Prioritize Immune-Related Nearest Genes Based on Association with Intra-Tumor Immune Cell Infiltration

We downloaded tumor bulk RNA-Seq gene expression data for 1084 breast, 494 prostate, 589 ovarian and 529 endometrial tumors profiled in The Cancer Genome Atlas (TCGA) PanCancer Atlas project from the cBioPortal [25]. Specifically, we used the log-transformed, RNA-Seq by expectation maximization (RSEM V2) and Z-score normalized data with the Z-scores computed relative to all samples. We subset these data to retain the nearest genes prioritized by the ImmPort and/or Enrichr analyses and used Spearman's rank correlation coefficient (ρ) to calculate the correlation between the expression of each of these genes and four T lymphocyte or myeloid white blood cell markers (*CD4*, *CD8A*, *CD11B* and *CD45*), the choice of these tumor immune cell infiltrate markers guided by and identical to the markers used by Fenaux et al. [6]. Genes with Spearman's $\rho > 0.5$ in the correlation analyses for at least one immune cell infiltrate marker across all four cancer types were defined as prioritized genes. Relative cell-specificity in the expression of the prioritized genes was evaluated using 12 breast, 6 prostate, 9 ovarian and 2 endometrial tumor single-cell RNA-Seq data sets available in the Tumor Immune Single-cell Hub 2 (TISCH2) database [26]. TISCH2 is a database of uniformly processed single-cell RNA-Seq data sets obtained from multiple cancer types and annotated by tumor microenvironment cell type. Specifically, we sought evidence that across the four cancer types, the prioritized genes had higher expression in tumor-infiltrating immune cells as compared to malignant, stromal, or other cell types within the tumor. Collectively, the purpose of these bulk and single-cell RNA-Seq analyses was to establish correlations in expression between the prioritized nearest genes and the intra-tumor immune response.

### 2.5. Functional Annotation to Link Prioritized Genes and Their Corresponding Lead SNPs

For the prioritized genes, we performed lookups of the corresponding lead SNPs in the OpenTargets Genetics database [27]. OpenTargets provided information on expression/splice/protein quantitative trait loci (e/s/p-QTLs), promoter capture Hi-C chromosome conformation and chromatin interactions and variant coding effect predictions [27]. This yielded functional genomic evidence that reinforced the status of the nearest gene as the most likely target of the lead SNP for the nearest genes prioritized by the combination of the immune-related gene annotation and intra-tumor bulk RNA-Seq expression immune marker correlation analyses. We also assessed the directionality of our findings using blood-based local or *cis*-eQTL data for 31,684 individuals from the eQTLGen consortium (*cis* being defined as genomic distance < 1 megabase between the eQTL SNP and the gene whose expression it regulates; [28]). Specifically, we assessed the direction of regulation of expression for each prioritized gene for the effect allele of the corresponding lead SNP that had opposite effects on autoimmune/autoinflammatory disease and cancer. For genes not available in eQTLGen, we performed a lookup of the Genotype Tissue Expression (GTEx) project whole blood eQTL data [29]. For the non-coding and non-synonymous lead SNPs, we also investigated the functional regulatory mechanisms through which the SNPs were most likely to alter gene expression using chromatin state data available in the RegulomeDB version 2 database [30].

### 2.6. Evaluating the Druggability of Proteins Encoded by the Prioritized Genes

We examined the druggability of the proteins encoded by the prioritized genes using the DrugnomeAI tool version 1 [31]. DrugnomeAI is a stochastic, semi-supervised machine learning framework recently developed to predict the druggability of proteins encoded by the human exome. Within this framework, genes encoding proteins that are established targets of known drugs are labeled and 324 gene-level predictors curated from

15 data sources are modeled using an ensemble of classifiers to generate predictions of whether a particular unlabeled gene/protein is likely to be therapeutically targetable. The DrugnomeAI predictions take the form of percentile scores (higher being better, with scores > 90th percentile generally deemed "high probability" candidates) ranking each gene/protein relative to all other genes/proteins for targeting by each of three specific drug modalities: small molecules, antibodies and PROTACs. The framework also provides oncology-specific prediction models for gene/protein targeting by small molecule- and antibody-based drugs.

## 3. Results

Our pairwise cross-disorder meta-analyses followed by linkage disequilibrium-based clumping to identify independent lead SNPs yielded 80 overall breast cancer, 83 ER-positive breast cancer, 35 ER-negative breast cancer, 27 ovarian cancer, 20 high-grade serous ovarian cancer, 101 prostate cancer and 52 endometrial cancer susceptibility alleles that were associated with the cancer at $p < 10^{-3}$ and had an opposite effect on, and $p < 10^{-3}$ association with, at least one of the seven autoimmune/autoinflammatory diseases (Supplementary Table S2 for total lead SNPs by analysis, Supplementary Tables S3–S9 for details of lead SNPs from each pairwise meta-analysis). Each of these 398 lead SNPs reached genome-wide significance ($p < 5 \times 10^{-8}$) in the pairwise cross-disorder meta-analysis where it was identified and demonstrated little statistical evidence of heterogeneity in effect sizes themselves (Cochran's Q test $p > 0.05$) though the direction of effect across cancer and autoimmune disease were opposite. These 398 lead SNPs consisted of 312 unique SNPs including 244 that were identified in only one paired cancer-autoimmune/autoinflammatory disease meta-analysis and 68 SNPs that were identified in multiple paired meta-analyses.

Annotating the lead SNPs identified from the pairwise cancer-autoimmune/autoinflammatory disease meta-analyses with their nearest genes using FUMA and then overlapping the nearest gene list with immune-related genes from ImmPort (Supplementary Table S10) and Enrichr (Supplementary Table S11) revealed a total of 32 genes that were a nearest gene *and* an immune-function-related gene (Table 1; 16 ImmPort genes, 20 Enrichr genes; 4 overlapping between the methods). The expression of five of these 32 genes (*IRF1*, *IKZF1*, *SPI1*, *SH2B3* and *LAT*) were strongly correlated (Spearman's $\rho > 0.5$) with the expression of at least one tumor immune cell infiltrate marker (*CD4*, *CD8A*, *CD11B* and *CD45*) in all four cancer types (breast, prostate, ovarian and endometrial) in bulk RNA-Seq data from TCGA (Figure 1). In fact, all five of these genes had a minimum $\rho \geq 0.37$ for all four intra-tumor T lymphocyte/myeloid cell markers across all four cancers (Figure 1). In general, all five genes were more highly expressed in the immune cell compartment (versus in malignant, stromal and other cells) in breast, prostate, ovarian and endometrial tumor single-cell RNA-Seq data sets (Figure 2).

**Table 1.** Immune-related genes among the nearest genes for lead SNPs identified in our cross-disorder meta-analyses with opposite allelic effects on autoimmune/autoinflammatory disease and cancer. Full results of the ImmPort and Enrichr analyses are provided in Supplementary Tables S10 and S11 and genes overlapping between ImmPort and Enrichr are highlighted with ** and bold font.

| Genes | ImmPort | Enrichr | ImmPort Category/Enrichr Pathway |
|---|---|---|---|
| *ADCY3* | | ✓ | Human T-cell leukemia virus 1 infection |
| *ADCY9* | | ✓ | Human T-cell leukemia virus 1 infection |
| *ATM* | | ✓ | Human T-cell leukemia virus 1 infection |
| *CCL11* | ✓ | | Cytokines/Antimicrobials/Chemokines |

**Table 1.** *Cont.*

| Genes | ImmPort | Enrichr | ImmPort Category/Enrichr Pathway |
|---|---|---|---|
| *CCL28* | ✓ | | Cytokines/Antimicrobials/Chemokines |
| *CGA* | ✓ | | Cytokines |
| *CRHR1* | ✓ | | Cytokine receptors |
| *CSK* | ✓ | | Antimicrobials |
| *DEFB136* | ✓ | | Antimicrobials |
| *GABBR1* | | ✓ | Inflammatory Response |
| *HELZ2* | | ✓ | Interferon α Response |
| *IFITM2* | | ✓ | Interferon α/β signaling R-HSA-909733/Interferon α Response |
| *IKZF1* | | ✓ | Development of pulmonary dendritic cells and macrophage subsets WP3892 |
| *IP6K2* | | ✓ | Interferon α/β signaling R-HSA-909733 |
| *IRF1* | ✓** | ✓** | Antimicrobials/Interferon α/β signaling R-HSA-909733/Interferon α Response |
| *IRF6* | | ✓ | Interferon α/β signaling R-HSA-909733/Inflammatory Response |
| *ITGB3* | | ✓ | Inflammatory Response |
| *ITGB8* | | ✓ | Inflammatory Response |
| *LAT* | ✓** | ✓** | Natural killer cell cytotoxicity/TCR signaling pathway/Modulators of TCR signaling and T cell activation WP5072 |
| *MAPT* | ✓ | | Antimicrobials |
| *NFATC1* | ✓** | ✓** | Natural killer cell cytotoxicity/TCR signaling pathway/BCR signaling pathway/Human T-cell leukemia virus 1 infection |
| *NR3C1* | ✓ | | Cytokine receptors |
| *PDK1* | ✓ | | TCR signaling pathway |
| *PIK3R1* | ✓** | ✓** | Natural killer cell cytotoxicity/TCR signaling pathway/BCR signaling pathway/Modulators of TCR signaling and T cell activation WP5072/Human T-cell leukemia virus 1 infection |
| *PPARG* | ✓ | | Cytokine receptors/Antimicrobials |
| *RASA2* | | ✓ | Natural killer cell cytotoxicity/TCR signaling pathway/BCR signaling pathway/Modulators of TCR signaling and T cell activation WP5072/Human T-cell leukemia virus 1 infection |
| *SH2B3* | | ✓ | TCR signaling pathway/Modulators of TCR signaling and T cell activation WP5072 |
| *SKAP1* | | ✓ | TCR signaling pathway |
| *SPI1* | | ✓ | Development of pulmonary dendritic cells and macrophage subsets WP3892/Human T-cell leukemia virus 1 infection |
| *TCF7L2* | ✓ | | Antimicrobials |
| *TERT* | | ✓ | Human T-cell leukemia virus 1 infection |
| *TRIM27* | ✓ | | Antimicrobials |

| Cancer | Breast | | | | Prostate | | | | Ovarian | | | | Endometrial | | | |
|---|---|---|---|---|---|---|---|---|---|---|---|---|---|---|---|---|
| Immune marker / Gene expression | *CD4* | *CD8A* | *CD11B* | *CD45* | *CD4* | *CD8A* | *CD11B* | *CD45* | *CD4* | *CD8A* | *CD11B* | *CD45* | *CD4* | *CD8A* | *CD11B* | *CD45* |
| *ADCY3* | 0.21 | 0.21 | 0.14 | 0.20 | 0.52 | 0.46 | 0.59 | 0.48 | 0.07 | 0.11 | 0.15 | 0.11 | 0.02 | 0.06 | 0.10 | 0.10 |
| *ADCY9* | −0.08 | −0.13 | 0.02 | −0.05 | 0.40 | 0.23 | 0.49 | 0.37 | 0.21 | 0.16 | 0.31 | 0.26 | 0.07 | 0.11 | 0.14 | 0.12 |
| *ATM* | 0.32 | 0.25 | 0.33 | 0.52 | 0.24 | 0.18 | 0.29 | 0.47 | 0.01 | −0.14 | 0.03 | 0.03 | 0.08 | 0.07 | −0.06 | 0.26 |
| *CCL11* | 0.49 | 0.41 | 0.34 | 0.44 | 0.43 | 0.36 | 0.38 | 0.33 | 0.47 | 0.49 | 0.48 | 0.58 | 0.15 | 0.30 | 0.08 | 0.24 |
| *CCL28* | 0.08 | 0.13 | 0.02 | 0.12 | 0.35 | 0.39 | 0.36 | 0.34 | −0.05 | 0.02 | −0.01 | −0.01 | 0.01 | −0.10 | 0.00 | −0.07 |
| *CGA* | −0.10 | −0.08 | −0.14 | −0.09 | −0.06 | 0.05 | −0.07 | −0.06 | −0.07 | −0.02 | −0.04 | −0.05 | −0.27 | −0.33 | −0.28 | −0.23 |
| *CRHR1* | 0.07 | 0.12 | 0.06 | 0.07 | 0.22 | 0.32 | 0.28 | 0.12 | −0.08 | −0.05 | −0.04 | −0.06 | 0.06 | 0.03 | 0.01 | 0.01 |
| *CSK* | 0.39 | 0.39 | 0.17 | 0.24 | −0.18 | −0.12 | −0.26 | −0.30 | 0.25 | 0.14 | 0.21 | 0.19 | 0.14 | 0.20 | 0.23 | 0.07 |
| *DEFB136* | 0.06 | 0.04 | 0.04 | 0.06 | 0.00 | 0.06 | 0.00 | −0.02 | NA | NA | NA | NA | NA | NA | NA | NA |
| *GABBR1* | −0.02 | 0.06 | 0.04 | −0.03 | 0.00 | 0.12 | 0.03 | −0.04 | −0.03 | −0.09 | 0.01 | −0.05 | −0.05 | −0.05 | −0.05 | −0.09 |
| *HELZ2* | 0.22 | 0.24 | 0.12 | 0.21 | 0.24 | 0.15 | 0.24 | 0.30 | 0.14 | 0.12 | 0.21 | 0.18 | −0.01 | 0.03 | 0.08 | 0.06 |
| *IFITM2* | 0.10 | 0.03 | 0.09 | −0.02 | 0.39 | 0.40 | 0.37 | 0.21 | 0.18 | 0.08 | 0.12 | 0.15 | 0.28 | 0.09 | 0.28 | 0.09 |
| *IKZF1* | 0.86 | 0.83 | 0.59 | 0.95 | 0.46 | 0.46 | 0.43 | 0.56 | 0.80 | 0.69 | 0.79 | 0.87 | 0.79 | 0.76 | 0.66 | 0.86 |
| *IP6K2* | −0.19 | −0.08 | −0.17 | −0.29 | −0.26 | −0.18 | −0.34 | −0.35 | −0.19 | −0.21 | −0.29 | −0.28 | −0.08 | −0.15 | −0.09 | −0.30 |
| *IRF1* | 0.64 | 0.68 | 0.50 | 0.61 | 0.54 | 0.62 | 0.47 | 0.50 | 0.49 | 0.49 | 0.43 | 0.51 | 0.59 | 0.55 | 0.50 | 0.54 |
| *IRF6* | −0.13 | −0.16 | 0.04 | −0.04 | 0.17 | 0.12 | 0.25 | 0.30 | −0.09 | −0.18 | −0.06 | −0.13 | −0.04 | −0.20 | 0.04 | 0.01 |
| *ITGB3* | 0.24 | 0.02 | 0.27 | 0.30 | 0.32 | 0.29 | 0.48 | 0.43 | 0.13 | 0.05 | 0.24 | 0.21 | 0.04 | 0.07 | 0.16 | 0.20 |
| *ITGB8* | 0.06 | 0.03 | 0.20 | 0.13 | 0.32 | 0.40 | 0.42 | 0.45 | 0.06 | 0.00 | 0.15 | 0.11 | −0.07 | −0.09 | −0.03 | 0.11 |
| *LAT* | 0.67 | 0.75 | 0.42 | 0.61 | 0.54 | 0.57 | 0.46 | 0.40 | 0.49 | 0.58 | 0.44 | 0.55 | 0.49 | 0.51 | 0.37 | 0.39 |
| *MAPT* | −0.26 | −0.20 | −0.10 | −0.24 | −0.16 | −0.19 | −0.13 | −0.12 | −0.14 | −0.07 | −0.12 | −0.14 | −0.05 | 0.00 | −0.09 | −0.05 |
| *NFATC1* | 0.23 | 0.19 | 0.22 | 0.18 | 0.23 | 0.25 | 0.25 | 0.13 | 0.33 | 0.34 | 0.40 | 0.39 | 0.19 | 0.19 | 0.23 | 0.10 |
| *NR3C1* | 0.32 | 0.26 | 0.23 | 0.44 | 0.34 | 0.35 | 0.42 | 0.48 | 0.38 | 0.34 | 0.42 | 0.46 | 0.30 | 0.33 | 0.20 | 0.44 |
| *PDK1* | 0.13 | 0.10 | 0.08 | 0.23 | −0.05 | −0.16 | −0.04 | 0.10 | −0.15 | −0.08 | −0.11 | −0.11 | −0.21 | −0.08 | −0.18 | 0.04 |
| *PIK3R1* | 0.13 | 0.14 | 0.17 | 0.25 | 0.30 | 0.29 | 0.39 | 0.47 | −0.10 | −0.15 | −0.04 | −0.10 | 0.19 | 0.06 | 0.13 | 0.20 |
| *PPARG* | 0.30 | 0.32 | 0.19 | 0.30 | 0.30 | 0.22 | 0.30 | 0.22 | 0.34 | 0.39 | 0.34 | 0.42 | −0.03 | −0.03 | −0.06 | 0.00 |
| *RASA2* | 0.19 | 0.12 | 0.23 | 0.41 | 0.29 | 0.11 | 0.36 | 0.50 | 0.11 | −0.02 | 0.21 | 0.17 | −0.09 | 0.00 | −0.10 | 0.23 |
| *SH2B3* | 0.65 | 0.45 | 0.48 | 0.67 | 0.68 | 0.48 | 0.72 | 0.69 | 0.72 | 0.43 | 0.78 | 0.73 | 0.53 | 0.39 | 0.50 | 0.61 |
| *SKAP1* | 0.06 | 0.15 | 0.08 | 0.08 | 0.74 | 0.67 | 0.64 | 0.65 | 0.00 | 0.12 | −0.10 | −0.03 | 0.39 | 0.23 | 0.30 | 0.22 |
| *SPI1* | 0.87 | 0.58 | 0.67 | 0.64 | 0.87 | 0.64 | 0.79 | 0.67 | 0.90 | 0.66 | 0.85 | 0.89 | 0.87 | 0.60 | 0.82 | 0.66 |
| *TCF7L2* | 0.16 | 0.20 | 0.17 | 0.20 | 0.22 | 0.23 | 0.24 | 0.30 | 0.00 | −0.11 | −0.04 | −0.10 | −0.01 | 0.00 | −0.03 | 0.04 |
| *TERT* | 0.01 | 0.06 | −0.03 | −0.02 | −0.15 | −0.13 | −0.21 | −0.16 | −0.11 | −0.17 | −0.07 | −0.17 | −0.18 | −0.05 | −0.12 | −0.19 |
| *TRIM27* | −0.07 | 0.02 | −0.12 | −0.07 | −0.30 | −0.23 | −0.36 | −0.37 | −0.12 | −0.19 | −0.10 | −0.13 | 0.06 | −0.07 | 0.15 | −0.09 |

**Figure 1.** Matrix of expression correlations between immune genes identified by the cross-disorder GWAS meta-analyses and anti-tumor immune infiltrate markers in tumor bulk RNA-Seq data. The numbers shown are Spearman's rank correlation coefficients (ρ) for correlation in tumor bulk RNA-Seq-based expression levels between the 32 immune-related genes and four T lymphocyte or myeloid cell markers in TCGA breast, prostate, ovarian and endometrial cancers. Each of the 32 genes was the nearest gene for a genome-wide significant lead SNP identified in the pairwise meta-analyses with opposite allelic effects on autoimmune/autoinflammatory disease and cancer. Five genes, with corresponding rows outlined by black borders, were strongly correlated (Spearman's $\rho > 0.5$) with at least one of the four anti-tumor immune infiltrate markers in all four TCGA cancer cohorts evaluated.

OpenTargets annotation of the cross-disorder meta-analysis lead SNPs corresponding to the five genes (*IRF1*, *IKZF1*, *SPI1*, *SH2B3* and *LAT*) showed that all five lead SNPs were eQTLs and/or sQTLs for their nearest genes (Table 2). Furthermore, promoter capture Hi-C interactions connected the lead SNPs rs10230978 to *IKZF1* and rs3184504 to *SH2B3*, while the lead SNP rs3740688 was a missense variant (p.Trp262Arg) in *SPI1* (Table 2). SNP rs10230978 is an intergenic variant with *IKZF1* as its nearest gene and as per RegulomeDB lies in an active enhancer in CD14+ monocytes, natural killer cells, neutrophils, B cells and naive B cells. Variant rs3184504 is a nonsynonymous exonic SNP in *SH2B3* and lies in a genic enhancer in T-helper 1, T-helper 2 and T-helper 17 cells. SNP rs2070721 lies in the active transcription start site of *IRF1* in T-helper 1, T-helper 2 and T-helper 17 cells while rs4788115 lies in a genic enhancer of *LAT* in T-helper 1, T-helper 2 and T-helper 17 cells, and likely regulate expression of their target genes via enhancer-promoter interactions. We used forest plots to visualize the genetic associations between the cross-disorder meta-analysis lead SNPs corresponding to the five genes and the cancer types and autoimmune/autoinflammatory diseases with which they were associated (Figure 3A). For rs2070721, rs3740688 and rs4788115, the allele that increased cancer risk also increased expression of IRF1, SPI1 and LAT, respectively, in the eQTLGen data (Figure 3B and Supplementary Table S12). For rs10230978 and rs3184504, the allele that increased cancer risk decreased the expression of IKZF1 and SH2B3, respectively (Figure 3B and Supplementary Table S12). Finally, DrugnomeAI predictions indicated that it was highly probable (percentile scores $\geq 94$) that the proteins encoded by *IRF1*, *SPI1*, *SH2B3* and *LAT* were targetable via antibody drugs while *IKZF1* received a high probability (percentile score = 93) for its protein product likely being targetable by PROTACs (Table 2).

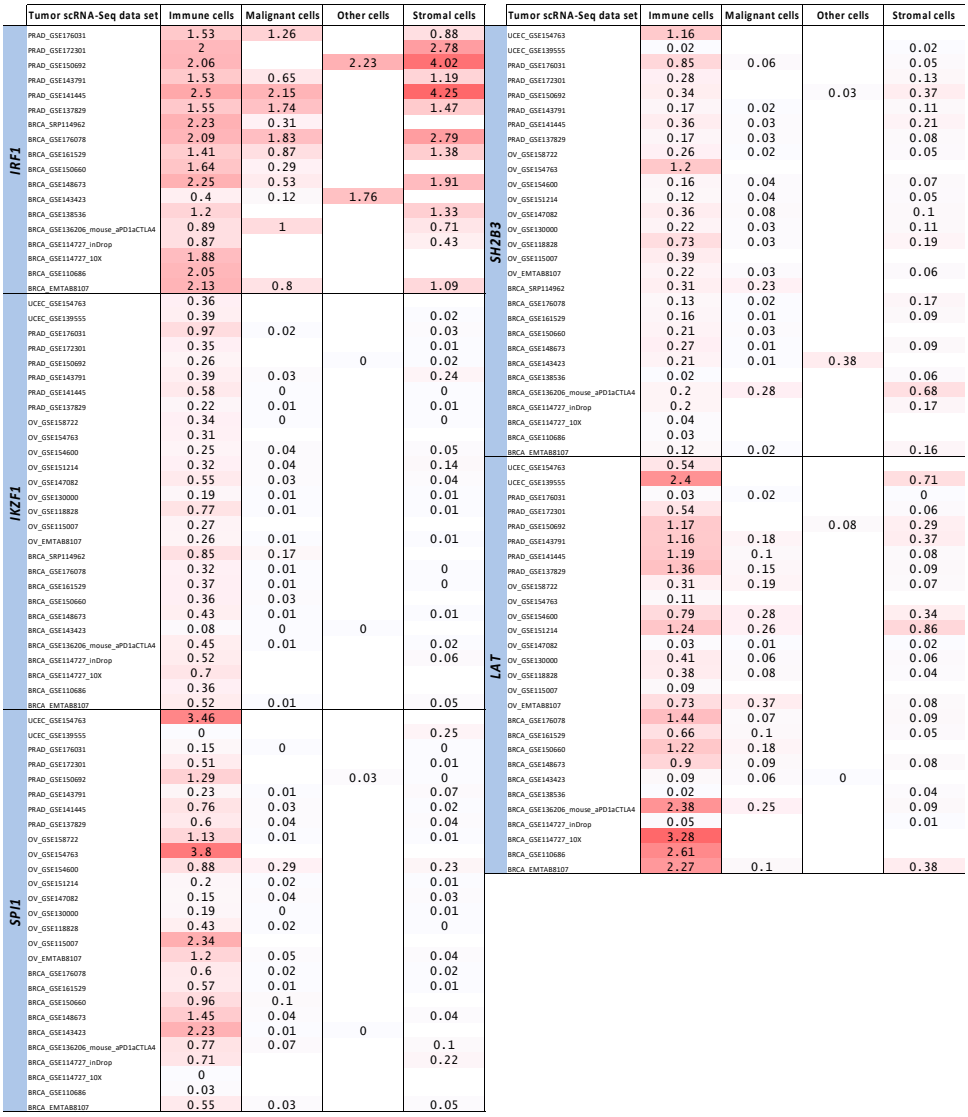

| | Tumor scRNA-Seq data set | Immune cells | Malignant cells | Other cells | Stromal cells |
|---|---|---|---|---|---|
| *IRF1* | PRAD_GSE176031 | 1.53 | 1.26 | | 0.88 |
| | PRAD_GSE172301 | 2 | | | 2.78 |
| | PRAD_GSE150692 | 2.06 | | 2.23 | 4.02 |
| | PRAD_GSE143791 | 1.53 | 0.65 | | 1.19 |
| | PRAD_GSE141445 | 2.5 | 2.15 | | 4.25 |
| | PRAD_GSE137829 | 1.55 | 1.74 | | 1.47 |
| | BRCA_SRP114962 | 2.23 | 0.31 | | |
| | BRCA_GSE176078 | 2.09 | 1.83 | | 2.79 |
| | BRCA_GSE161529 | 1.41 | 0.87 | | 1.38 |
| | BRCA_GSE150660 | 1.64 | 0.29 | | |
| | BRCA_GSE148673 | 2.25 | 0.53 | | 1.91 |
| | BRCA_GSE143423 | 0.4 | 0.12 | 1.76 | |
| | BRCA_GSE138536 | 1.2 | | | 1.33 |
| | BRCA_GSE136206_mouse_aPD1aCTLA4 | 0.89 | 1 | | 0.71 |
| | BRCA_GSE114727_inDrop | 0.87 | | | 0.43 |
| | BRCA_GSE114727_10X | 1.88 | | | |
| | BRCA_GSE110686 | 2.05 | | | |
| | BRCA_EMTAB8107 | 2.13 | 0.8 | | 1.09 |
| *IKZF1* | UCEC_GSE154763 | 0.36 | | | |
| | UCEC_GSE139555 | 0.39 | | | 0.02 |
| | PRAD_GSE176031 | 0.97 | 0.02 | | 0.03 |
| | PRAD_GSE172301 | 0.35 | | | 0.01 |
| | PRAD_GSE150692 | 0.26 | | 0 | 0.02 |
| | PRAD_GSE143791 | 0.39 | 0.03 | | 0.24 |
| | PRAD_GSE141445 | 0.58 | 0 | | 0 |
| | PRAD_GSE137829 | 0.22 | 0.01 | | 0.01 |
| | OV_GSE158722 | 0.34 | 0 | | 0 |
| | OV_GSE154763 | 0.31 | | | |
| | OV_GSE154600 | 0.25 | 0.04 | | 0.05 |
| | OV_GSE151214 | 0.32 | 0.04 | | 0.14 |
| | OV_GSE147082 | 0.55 | 0.03 | | 0.04 |
| | OV_GSE130000 | 0.19 | 0.01 | | 0.01 |
| | OV_GSE118828 | 0.77 | 0.01 | | 0.01 |
| | OV_GSE115007 | 0.27 | | | |
| | OV_EMTAB8107 | 0.26 | 0.01 | | 0.01 |
| | BRCA_SRP114962 | 0.85 | 0.17 | | |
| | BRCA_GSE176078 | 0.32 | 0.01 | | 0 |
| | BRCA_GSE161529 | 0.37 | 0.01 | | 0 |
| | BRCA_GSE150660 | 0.36 | 0.03 | | |
| | BRCA_GSE148673 | 0.43 | 0.01 | | 0.01 |
| | BRCA_GSE143423 | 0.08 | 0 | 0 | |
| | BRCA_GSE136206_mouse_aPD1aCTLA4 | 0.45 | 0.01 | | 0.02 |
| | BRCA_GSE114727_inDrop | 0.52 | | | 0.06 |
| | BRCA_GSE114727_10X | 0.7 | | | |
| | BRCA_GSE110686 | 0.36 | | | |
| | BRCA_EMTAB8107 | 0.52 | 0.01 | | 0.05 |
| *SPI1* | UCEC_GSE154763 | 3.46 | | | |
| | UCEC_GSE139555 | 0 | | | 0.25 |
| | PRAD_GSE176031 | 0.15 | 0 | | 0 |
| | PRAD_GSE172301 | 0.51 | | | 0.01 |
| | PRAD_GSE150692 | 1.29 | | 0.03 | 0 |
| | PRAD_GSE143791 | 0.23 | 0.01 | | 0.07 |
| | PRAD_GSE141445 | 0.76 | 0.03 | | 0.02 |
| | PRAD_GSE137829 | 0.6 | 0.04 | | 0.04 |
| | OV_GSE158722 | 1.13 | 0.01 | | 0.01 |
| | OV_GSE154763 | 3.8 | | | |
| | OV_GSE154600 | 0.88 | 0.29 | | 0.23 |
| | OV_GSE151214 | 0.2 | 0.02 | | 0.01 |
| | OV_GSE147082 | 0.15 | 0.04 | | 0.03 |
| | OV_GSE130000 | 0.19 | 0 | | 0.01 |
| | OV_GSE118828 | 0.43 | 0.02 | | 0 |
| | OV_GSE115007 | 2.34 | | | |
| | OV_EMTAB8107 | 1.2 | 0.05 | | 0.04 |
| | BRCA_GSE176078 | 0.6 | 0.02 | | 0.02 |
| | BRCA_GSE161529 | 0.57 | 0.01 | | 0.01 |
| | BRCA_GSE150660 | 0.96 | 0.1 | | |
| | BRCA_GSE148673 | 1.45 | 0.04 | | 0.04 |
| | BRCA_GSE143423 | 2.23 | 0.01 | 0 | |
| | BRCA_GSE136206_mouse_aPD1aCTLA4 | 0.77 | 0.07 | | 0.1 |
| | BRCA_GSE114727_inDrop | 0.71 | | | 0.22 |
| | BRCA_GSE114727_10X | 0 | | | |
| | BRCA_GSE110686 | 0.03 | | | |
| | BRCA_EMTAB8107 | 0.55 | 0.03 | | 0.05 |

| | Tumor scRNA-Seq data set | Immune cells | Malignant cells | Other cells | Stromal cells |
|---|---|---|---|---|---|
| *SH2B3* | UCEC_GSE154763 | 1.16 | | | |
| | UCEC_GSE139555 | 0.02 | | | 0.02 |
| | PRAD_GSE176031 | 0.85 | 0.06 | | 0.05 |
| | PRAD_GSE172301 | 0.28 | | | 0.13 |
| | PRAD_GSE150692 | 0.34 | | 0.03 | 0.37 |
| | PRAD_GSE143791 | 0.17 | 0.02 | | 0.11 |
| | PRAD_GSE141445 | 0.36 | 0.03 | | 0.21 |
| | PRAD_GSE137829 | 0.17 | 0.03 | | 0.08 |
| | OV_GSE158722 | 0.26 | 0.02 | | 0.05 |
| | OV_GSE154763 | 1.2 | | | |
| | OV_GSE154600 | 0.16 | 0.04 | | 0.07 |
| | OV_GSE151214 | 0.12 | 0.04 | | 0.05 |
| | OV_GSE147082 | 0.36 | 0.08 | | 0.1 |
| | OV_GSE130000 | 0.22 | 0.03 | | 0.11 |
| | OV_GSE118828 | 0.73 | 0.03 | | 0.19 |
| | OV_GSE115007 | 0.39 | | | |
| | OV_EMTAB8107 | 0.22 | 0.03 | | 0.06 |
| | BRCA_SRP114962 | 0.31 | 0.23 | | |
| | BRCA_GSE176078 | 0.13 | 0.02 | | 0.17 |
| | BRCA_GSE161529 | 0.16 | 0.01 | | 0.09 |
| | BRCA_GSE150660 | 0.21 | 0.03 | | |
| | BRCA_GSE148673 | 0.27 | 0.01 | | 0.09 |
| | BRCA_GSE143423 | 0.21 | 0.01 | 0.38 | |
| | BRCA_GSE138536 | 0.02 | | | 0.06 |
| | BRCA_GSE136206_mouse_aPD1aCTLA4 | 0.2 | 0.28 | | 0.68 |
| | BRCA_GSE114727_inDrop | 0.2 | | | 0.17 |
| | BRCA_GSE114727_10X | 0.04 | | | |
| | BRCA_GSE110686 | 0.03 | | | |
| | BRCA_EMTAB8107 | 0.12 | 0.02 | | 0.16 |
| *LAT* | UCEC_GSE154763 | 0.54 | | | |
| | UCEC_GSE139555 | 2.4 | | | 0.71 |
| | PRAD_GSE176031 | 0.03 | 0.02 | | 0 |
| | PRAD_GSE172301 | 0.54 | | | 0.06 |
| | PRAD_GSE150692 | 1.17 | | 0.08 | 0.29 |
| | PRAD_GSE143791 | 1.16 | 0.18 | | 0.37 |
| | PRAD_GSE141445 | 1.19 | 0.1 | | 0.08 |
| | PRAD_GSE137829 | 1.36 | 0.15 | | 0.09 |
| | OV_GSE158722 | 0.31 | 0.19 | | 0.07 |
| | OV_GSE154763 | 0.11 | | | |
| | OV_GSE154600 | 0.79 | 0.28 | | 0.34 |
| | OV_GSE151214 | 1.24 | 0.26 | | 0.86 |
| | OV_GSE147082 | 0.03 | 0.01 | | 0.02 |
| | OV_GSE130000 | 0.41 | 0.06 | | 0.06 |
| | OV_GSE118828 | 0.38 | 0.08 | | 0.04 |
| | OV_GSE115007 | 0.09 | | | |
| | OV_EMTAB8107 | 0.73 | 0.37 | | 0.08 |
| | BRCA_GSE176078 | 1.44 | 0.07 | | 0.09 |
| | BRCA_GSE161529 | 0.66 | 0.1 | | 0.05 |
| | BRCA_GSE150660 | 1.22 | 0.18 | | |
| | BRCA_GSE148673 | 0.9 | 0.09 | | 0.08 |
| | BRCA_GSE143423 | 0.09 | 0.06 | 0 | |
| | BRCA_GSE138536 | 0.02 | | | 0.04 |
| | BRCA_GSE136206_mouse_aPD1aCTLA4 | 2.38 | 0.25 | | 0.09 |
| | BRCA_GSE114727_inDrop | 0.05 | | | 0.01 |
| | BRCA_GSE114727_10X | 3.28 | | | |
| | BRCA_GSE110686 | 2.61 | | | |
| | BRCA_EMTAB8107 | 2.27 | 0.1 | | 0.38 |

**Figure 2.** Lineage-wise expression of the five prioritized genes in breast, prostate, ovarian and endometrial tumor single-cell RNA-Seq data. The five genes represent the final targets prioritized by the analytic pipeline from the cross-disorder pairwise meta-analyses, to lead SNP and nearest gene mapping, to the ImmPort, Enrichr and TCGA analyses. The expression of each gene was evaluated across immune, malignant, stromal and other cellular lineages in breast, prostate, ovarian and endometrial tumor single-cell RNA-Seq data sets available in the TISCH2 database. Values shown are in log(transcripts per million/10 + 1).

**Table 2.** OpenTargets evidence linking lead SNPs to nearest genes and DrugnomeAI percentile scores for the probability that the protein encoded by a gene is "druggable" for the five genes prioritized by our analytic pipeline (cross-disorder GWAS meta-analyses + nearest gene/immune-related function annotation + tumor bulk and single-cell RNA-seq analyses).

| | | OpenTargets Lead SNP-to-Gene Evidence | | | | DrugnomeAI Percentile Scores for Druggability | | | | |
|---|---|---|---|---|---|---|---|---|---|---|
| **Lead SNP** | **Gene** | **sQTL** | **eQTL** | **PCHi-C** | **VEP** | **Oncology Specific-Antibody** | **Oncology Specific-Small Molecule** | **Small Molecule** | **Antibody** | **PROTAC** |
| rs2070721 | *IRF1* | Yes | Yes | | intronic variant | 92 | 76 | 75 | 95 | 91 |
| rs10230978 | *IKZF1* | | Yes | Yes | | 89 | 87 | 85 | 88 | 93 |

**Table 2.** *Cont.*

| | | | OpenTargets Lead SNP-to-Gene Evidence | | | DrugnomeAI Percentile Scores for Druggability | | | | |
|---|---|---|---|---|---|---|---|---|---|---|
| **Lead SNP** | **Gene** | **sQTL** | **eQTL** | **PCHi-C** | **VEP** | **Oncology Specific-Antibody** | **Oncology Specific-Small Molecule** | **Small Molecule** | **Antibody** | **PROTAC** |
| rs3740688 | *SPI1* | | Yes | | missense variant | 96 | 82 | 81 | 93 | 88 |
| rs3184504 | *SH2B3* | | Yes | Yes | | 94 | 89 | 89 | 96 | 95 |
| rs4788115 | *LAT* | Yes | | | intronic variant | 97 | 85 | 84 | 96 | 95 |

Abbreviations: s/eQTL (splicing/expression quantitative trait locus); PCHi-C (promoter capture Hi-C); VEP (variant effect prediction); PROTAC (proteolysis targeting chimera). Percentile scores > 95 (and >90 for PROTAC) are considered "high probability" as per the DrugnomeAI classification.

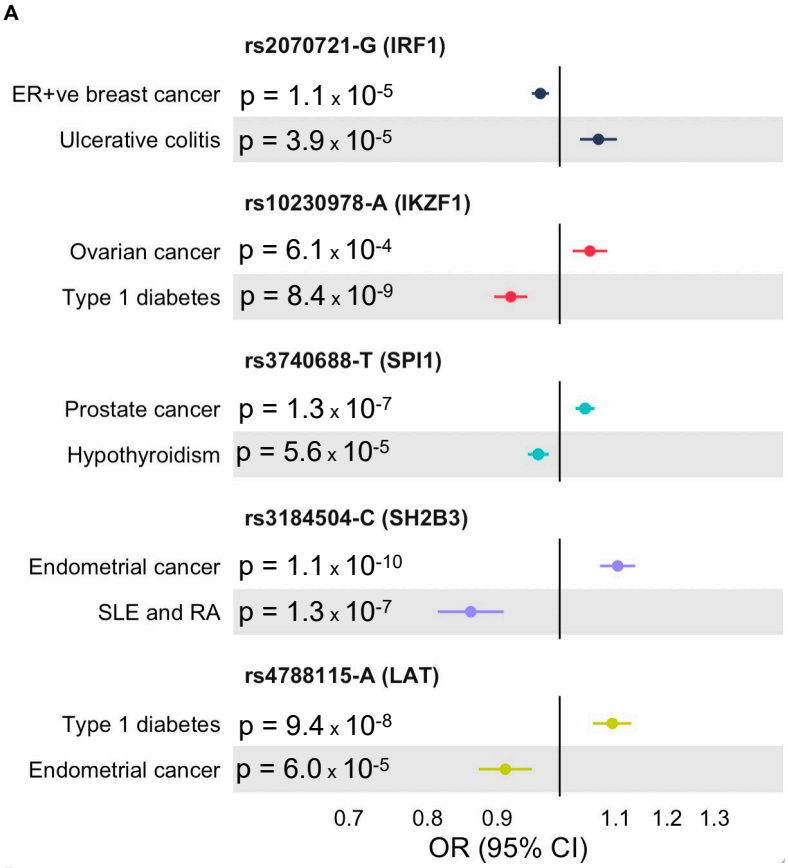


**B**

| SNP-effect allele | Phenotype | Z-score | *P*-value |
|---|---|---|---|
| rs2070721-G | ER+ve breast cancer | -4 | $1.1 \times 10^{-5}$ |
| | *IRF1* expression | -8 | $3.4 \times 10^{-15}$ |
| rs10230978-A | Ovarian cancer | 3 | $6.1 \times 10^{-4}$ |
| | *IKZF1* expression | -39 | $3.3 \times 10^{-310}$ |
| rs3740688-T | Prostate cancer | 5 | $1.3 \times 10^{-7}$ |
| | *SPI1* expression | 8 | $2.8 \times 10^{-15}$ |
| rs3184504-C | Endometrial cancer | 6 | $1.1 \times 10^{-10}$ |
| | *SH2B3* expression | -18 | $1.0 \times 10^{-68}$ |
| rs4788115-A | Endometrial cancer | -4 | $6.0 \times 10^{-5}$ |
| | *LAT* expression | -4 | $9.9 \times 10^{-5}$ |

**Figure 3.** Genetic association forest plots and gene expression associations for the lead SNPs near *IRF1*, *IKZF1*, *SPI1*, *SH2B3* and *LAT*: (**A**) For each lead SNP, the effect allele, nearest gene, *p*-value, odds ratio (OR) and 95% confidence interval (CI) are shown for the autoimmune/autoinflammatory

disease GWAS and cancer GWAS associations. The five genes represent the final targets prioritized by the analytic pipeline from the cross-disorder pairwise meta-analyses, to lead SNP and nearest gene mapping, to the ImmPort, Enrichr and TCGA analyses. For rs3184504-C, the association with SLE is shown while the association with RA is OR = 0.93; 95% CI: 0.89—0.95; $p = 3 \times 10^{-7}$; (**B**) For each lead SNP, the effect allele, Z-score and *p*-value are shown for the cancer association and for the expression (eQTL) association with the nearest gene.

## 4. Discussion

In this study, we have integrated GWAS data sets across seven autoimmune/autoinflammatory diseases and four cancer types and three cancer subtypes (that are typically immune "cold" tumors) spanning over 1.5 million individuals to identify common inherited polymorphisms associated with, and with opposite allelic effects on, cancer and autoimmune/autoinflammatory disease. By bringing together a comprehensive analytic pipeline that included lead SNP-to-nearest gene mapping to link the SNPs to their most probable effector genes, immune-related gene annotation for the nearest genes, correlation of immune-annotated nearest genes with anti-tumor immune response signatures in tumor bulk and single-cell RNA-Seq data, we prioritized five genes: *IRF1*, *IKZF1*, *SPI1*, *SH2B3* and *LAT*. The lead SNP corresponding to each of these genes was an eQTL for the gene and the proteins encoded by the five genes are potentially druggable candidates. Given all these findings, we highlight the five genes as candidate targets supported by a strong scientific rationale for future in-depth exploration in immuno-oncology drug development programs. Here, we discuss each gene in greater detail.

*IRF1* encodes interferon regulatory factor 1, a transcription factor that binds to interferon-stimulated response elements and plays a vital role in several aspects of the innate and adaptive immune response. IRF1 has been shown to upregulate *CD274* (that encodes PD-L1) expression in the tumor microenvironment and *IRF1* "knock-out" has been shown to render tumor cells more susceptible to CD8+ T cell-mediated killing [32,33]. Recently, a peptide inhibitor of IRF1's interaction with KAT8, a histone acetyltransferase and interaction partner of IRF1, has been shown to inhibit PD-L1 expression and improve the anti-tumor immune response both in vitro and in vivo [34], suggesting that targeting IRF1 or its interactions may represent a promising strategy for cancer immunotherapy. In keeping with these findings, our lead SNP rs2070721-G was associated with reductions in *IRF1* expression and ER-positive breast cancer risk and increased autoimmune/autoinflammatory disease (ulcerative colitis) risk.

*IKZF1* encodes an Ikaros family zinc finger transcription factor associated with chromatin remodeling. *IKZF1* expression is specific to the hematopoietic system and serves as a major regulator of lymphocyte differentiation, especially for CD4+ T cells and B cells. IKZF1 functions as a tumor suppressor in acute lymphoblastic leukemia [35]. In solid tumors, including prostate cancer, lack of *IKZF1* expression has been implicated as a mechanism for tumor immune evasion [36]. Moreover, overexpression of *IKZF1* has been associated with increased recruitment of anti-tumor immune cell infiltrates and sensitivity to anti-PD-1 and anti-CTLA4 therapy [36]. The directionality of our genetic epidemiological results was consistent with this biological background: the G allele of our meta-analysis lead SNP rs10230978 which was associated with elevated *IKZF1* expression was protective for ovarian cancer while increasing autoimmunity (type 1 diabetes) risk.

The *SPI1* proto-oncogene encodes a transcription factor that activates transcription during B-lymphoid and myeloid hematopoiesis. *SPI1* expression is strongly correlated with immune cell infiltration in clear cell renal cell cancer (ccRCC) and non-responders to anti-PD-1 therapy in the CheckMate 09, 10 and 25 ccRCC trials were more likely to overexpress *SPI1* than responders [37]. Similarly, in the Imvigor210 anti-PD-1/PD-L1 trial for urothelial

cancer, higher expression of *SPI1* and its regulatory targets was associated with significantly lower survival on immunotherapy [38]. Biologically and directionally consistent with these findings, in our analysis, the meta-analysis lead SNP rs3740688-T was associated with decreased autoimmune/autoinflammatory disease (Hashimoto's thyroiditis) risk, increased *SPI1* expression and increased prostate cancer risk.

*SH2B3* encodes the lymphocyte adapter protein, LNK. SH2B3 is a negative regulator of several key tyrosine kinases and cytokines, particularly JAK-STAT signaling, and has known tumor suppressor function in acute lymphoblastic leukemia and lung cancer [39,40]. SH2B3 is involved in the activation and expansion of CD8+ T cells [41,42]. In keeping with these prior biological observations, our analyses indicated that lead SNP rs3184504-C was associated with lower *SH2B3* expression, reduced autoimmune disease (RA and SLE) and higher endometrial cancer risk. In the context of *SH2B3*, it is worth noting that the lead SNP rs318450 is well known to be highly pleiotropic and the allele that decreases cancer risk is associated with increased cardiovascular disease risk probably mediated via an increase in blood pressure [43]. Currently approved immune checkpoint inhibitor treatments for cancer are also associated with hypertension and cardiotoxicities [44]. Thus, any drug development effort to target SH2B3 may have to find the right balance between inducing cancer suppression and cardiovascular/autoimmune toxicity.

*LAT* encodes the linker protein for activation of T cells. LAT is phosphorylated in response to activation of the T-cell antigen receptor (TCR) and in turn recruits other proteins into major functional complexes at the site of TCR engagement. Controlled modulation of LAT activity either through altered phosphorylation of LAT [45], or by amino acid substitution in the sequence of LAT [46], has been considered as a potential strategy to enhance the efficacy of adoptive immunotherapy in cancer using chimeric antigen receptor or CAR T-cells [47]. At the *LAT* locus, we found that lead SNP rs4788115-A was associated with reductions in both *LAT* expression and endometrial cancer risk while increasing autoimmune disease (type 1 diabetes) risk.

T1D, RA and autoimmune hypothyroidism are T-helper (Th) 1 dominant diseases, while SLE and ulcerative colitis are mediated by both Th1 and Th2 responses, with the Th2 response predominating in SLE [48]. Th1 cells, having been primed by tumor-antigen–loaded antigen-presenting cells (APCs) presenting via major histocompatibility complex (MHC) class II, express CD40 ligand and secrete interferon-$\gamma$ (IFN-$\gamma$). IFN-$\gamma$ (together with CD40L–CD40 interactions) licenses macrophages and dendritic cells by upregulating MHC I/II and co-stimulatory molecules. These licensed APCs then cross-present tumor antigens on MHC I to naive $CD8^+$ T cells—providing antigen, co-stimulation and cytokine signals—that drive their differentiation into cytotoxic T lymphocytes capable of directly killing tumor cells [49]. Historically, Th2-polarized responses were thought to dampen Th1-mediated cytotoxicity and favor tumor growth by skewing immunity toward interleukin (IL)-4/IL-13-driven humoral pathways. Recent work, however, shows that in certain cytokine and tissue contexts, Th2 cells can contribute to tumor rejection: they recruit and activate eosinophils (via IL-5/eotaxin) and, in some models, re-program macrophages to become tumoricidal, and activated Th2 cells themselves can acquire perforin/granzyme-dependent cytotoxicity. Thus, the net effect of Th2 immunity on cancer is highly context- and disease-dependent [50,51].

Of the 312 unique lead SNP loci with opposite allelic effects on at least one autoimmune/autoinflammatory disease and one cancer type/subtype, we chose to focus on 32 loci where the gene nearest to the lead SNP was clearly immune system-related. We then further prioritized 5 of these 32 genes since their tumor expression was strongly correlated with *CD4*, *CD8A*, *CD11B* or *CD45* tumor expression in all four cancers (breast, prostate, ovarian and endometrial). In this context, there are two points worth noting. First, while

the corresponding lead SNPs were associated with a risk of only one of the four cancers studied (for example, rs10240978-A had opposite effects on ovarian cancer and type 1 diabetes), the five corresponding target genes were correlated with tumor immune cell infiltration marker gene expression in all four cancers. This pattern was consistent with the previously published analyses that uncovered cross-disorder opposite effects at lead SNPs near *CD200*, *CD200R1* and *DOK2* where the germline genetic associations were confined to basal cell carcinoma but the tumor immune gene expression correlations encompassed several additional cancer types [6]. Pre-clinical data also showed that anti-CD200R1 antibody treatment had the potential to reverse immunosuppression in multiple cancer types [6].

Second, while we prioritized five of the 32 genes, the remainder of the 32 also contain genes of potential immuno-oncology interest. For example, lead SNP rs4795899-A (Supplementary Table S5) with nearest gene *CCL11* (Table 1) was associated with protection from Crohn's disease ($p = 7.7 \times 10^{-7}$) and increased risk of ER-negative breast cancer ($p = 5.9 \times 10^{-5}$) and was correlated with *CD4*, *CD8A*, *CD11B* and *CD45* expression in TCGA breast tumors with Spearman's ρ ranging from 0.34 to 0.49 (Figure 1). *CCL11* gene expression correlations were also modest in TCGA prostate and ovarian tumors but were much weaker in endometrial tumors and because our criteria for the top five genes were particularly stringent, requiring correlations with Spearman's $\rho > 0.5$ for at least one of *CD4*, *CD8A*, *CD11B* and *CD45* in all four cancer types, *CCL11* was not among our top five genes. *CCL11* encodes the major chemokine responsible for eosinophil recruitment and infiltration in the tumor microenvironment [52]. DPP4 post-translationally cleaves CCL11 to reduce eosinophil infiltration. DPP4 inhibition (using the anti-diabetic medication, sitagliptin) in a pre-clinical syngeneic mouse model of breast cancer has been shown to increase CCL11 levels, eosinophil infiltration and improve tumor control and was synergistic with immune checkpoint inhibition [53]. Finally, we emphasize that the results presented here are based on GWAS in individuals of European or predominantly European ancestry given the relative lack of ancestrally diverse GWAS data [54], which limits the statistical power of cross-ancestry analyses. Establishing the generalizability of our findings to other ancestral groups must be top priority in future studies. Future directions of investigation should also include evaluation of the SNPs identified in our work as single variant or polygenic predictors of immune checkpoint inhibitor response in cancer immunotherapy clinical trials and real-world cohorts [1,2,55].

Gene/protein targets supported by germline genetic association evidence have been shown to be over twice as likely to be successful at the pre-clinical and clinical phases of oncology drug development [56,57]. In the current study, we have provided large-scale germline genetic and tightly coupled immune, somatic and functional genomic evidence to support a deeper evaluation of the proteins encoded by *IRF1*, *IKZF1*, *SPI1*, *SH2B3* and *LAT* as possible targets for cancer immunotherapy, particularly in breast, prostate, ovarian and endometrial cancers where there is substantial unmet need for new immunotherapeutic targets.

**Supplementary Materials:** The following supporting information can be downloaded at: https://www.mdpi.com/article/10.3390/genes16050575/s1, Table S1: Overview of GWAS summary statistics data sets for the cancer types/subtypes and autoimmune/autoinflammatory diseases used in this study; Table S2: Number of lead SNPs identified in meta-analyses for each autoimmune/autoinflammatory disease-cancer pair; Table S3: Lead SNPs for breast cancer identified from meta-analysis with autoimmune/autoinflammatory disease GWAS; Table S4: Lead SNPs for ER + ve breast cancer identified from meta-analysis with autoimmune/autoinflammatory disease GWAS; Table S5: Lead SNPs for ER-ve breast cancer identified from meta-analysis with autoimmune/autoinflammatory disease GWAS; Table S6: Lead SNPs for ovarian cancer identified from meta-analysis with autoimmune/autoinflammatory disease GWAS; Table S7: Lead SNPs for high grade serous ovarian cancer

identified from meta-analysis with autoimmune/autoinflammatory disease GWAS; Table S8: Lead SNPs for prostate cancer identified from meta-analysis with autoimmune/autoinflammatory disease GWAS; Table S9: Lead SNPs for endometrial cancer identified from meta-analysis with autoimmune/autoinflammatory disease GWAS; Table S10: Genes nearest to lead SNPs that were classified as immune-related genes by ImmPort; Table S11: Immune-related pathways among the top 10 pathways identified by Enrichr gene set analysis; Table S12: eQTLGen consortium evidence linking lead SNPs to nearest genes for the five genes prioritized by the ImmPort/Enrichr + TCGA analyses.

**Author Contributions:** Conceptualization, S.P.K.; methodology, S.P.K., M.P.E. and J.M.S.; formal analysis, J.C.; resources, M.P.E., J.M.S. and S.P.K.; writing—original draft preparation, J.C.; writing—review and editing, M.P.E., J.M.S. and S.P.K.; visualization, J.C. and S.P.K.; supervision, S.P.K.; project administration, M.P.E., J.M.S. and S.P.K.; funding acquisition, M.P.E., J.M.S. and S.P.K. All authors have read and agreed to the published version of the manuscript.

**Funding:** This research was funded by UK Research and Innovation (grant number MR/T043202/2) and the National Institutes of Health (grant numbers R01CA259058, R01CA211574, RF1AG071170 and R01CA237318).

**Institutional Review Board Statement:** Not applicable.

**Informed Consent Statement:** Not applicable.

**Data Availability Statement:** All genome-wide association meta-analysis summary statistics used in this study are publicly available in the GWAS Catalog (https://www.ebi.ac.uk/gwas/home, accessed on 1 December 2022) via accession numbers GCST004132 (Crohn's disease), GCST004133 (ulcerative colitis), GCST002318 (rheumatoid arthritis), GCST003155 (systemic lupus erythematosus), GCST010571 (autoimmune thyroid disease), GCST005531 (multiple sclerosis), GCST90013445 (type 1 diabetes), GCST004988 (breast cancer), GCST006085 (prostate cancer), GCST004462 (ovarian cancer) and GCST006464 (endometrial cancer).

**Acknowledgments:** The results published here are in part based upon data generated by the TCGA Research Network: https://www.cancer.gov/tcga (accessed on 1 October 2023). We also thank the international consortia that have made the cancer, and autoimmune/autoinflammatory disease genome-wide association meta-analysis data sets used in this study publicly available.

**Conflicts of Interest:** The authors declare no conflicts of interest. The funders had no role in the design of the study; in the collection, analyses, or interpretation of data; in the writing of the manuscript; or in the decision to publish the results.

## Abbreviations

The following abbreviations are used in this manuscript:

| | |
|---|---|
| SNP | single nucleotide polymorphism |
| TCGA | The Cancer Genome Atlas |
| GWAS | genome-wide association study |
| PROTACs | proteolysis targeting chimeras |
| T1D | type 1 diabetes |
| RA | rheumatoid arthritis |
| HT | Hashimoto's thyroiditis |
| MS | multiple sclerosis |
| SLE | systemic lupus erythematosus |
| UC | ulcerative colitis |
| CD | Crohn's disease |
| ER | estrogen receptor |
| FUMA | Functional Mapping and Annotation |
| LD | linkage disequilibrium |
| KEGG | Kyoto Encyclopedia of Genes and Genomes |
| MSigDB | Molecular Signatures Database |

| | |
|---|---|
| TISCH2 | Tumor Immune Single-cell Hub 2 |
| eQTL | expression quantitative trait locus |
| RNA-Seq | ribonucleic acid-sequencing |
| RSEM | RNA-Seq by expectation maximization |
| OR | Odds ratio |
| CI | Confidence interval |

## References


1. Khan, Z.; Di Nucci, F.; Kwan, A.; Hammer, C.; Mariathasan, S.; Rouilly, V.; Carroll, J.; Fontes, M.; Ley Acosta, S.; Guardino, E.; et al. Polygenic Risk for Skin Autoimmunity Impacts Immune Checkpoint Blockade in Bladder Cancer. *Proc. Natl. Acad. Sci. USA* **2020**, *117*, 12288–12294. [CrossRef] [PubMed]
2. Khan, Z.; Hammer, C.; Carroll, J.; Di Nucci, F.; Acosta, S.L.; Maiya, V.; Bhangale, T.; Hunkapiller, J.; Mellman, I.; Albert, M.L.; et al. Genetic Variation Associated with Thyroid Autoimmunity Shapes the Systemic Immune Response to PD-1 Checkpoint Blockade. *Nat. Commun.* **2021**, *12*, 3355. [CrossRef] [PubMed]
3. Shahamatdar, S.; He, M.X.; Reyna, M.A.; Gusev, A.; AlDubayan, S.H.; Van Allen, E.M.; Ramachandran, S. Germline Features Associated with Immune Infiltration in Solid Tumors. *Cell Rep.* **2020**, *30*, 2900–2908.e4. [CrossRef]
4. Sayaman, R.W.; Saad, M.; Thorsson, V.; Hu, D.; Hendrickx, W.; Roelands, J.; Porta-Pardo, E.; Mokrab, Y.; Farshidfar, F.; Kirchhoff, T.; et al. Germline Genetic Contribution to the Immune Landscape of Cancer. *Immunity* **2021**, *54*, 367–386.e8. [CrossRef]
5. Liyanage, U.E.; MacGregor, S.; Bishop, D.T.; Shi, J.; An, J.; Ong, J.S.; Han, X.; Scolyer, R.A.; Martin, N.G.; Medland, S.E.; et al. Multi-Trait Genetic Analysis Identifies Autoimmune Loci Associated with Cutaneous Melanoma. *J. Investig. Dermatol.* **2022**, *142*, 1607–1616. [CrossRef]
6. Fenaux, J.; Fang, X.; Huang, Y.-M.; Melero, C.; Bonnans, C.; Lowe, E.L.; Palumbo, T.; Lay, C.; Yi, Z.; Zhou, A.; et al. 23ME-00610, a Genetically Informed, First-in-Class Antibody Targeting CD200R1 to Enhance Antitumor T Cell Function. *Oncoimmunology* **2023**, *12*, 2217737. [CrossRef]
7. Wu, B.; Zhang, B.; Li, B.; Wu, H.; Jiang, M. Cold and Hot Tumors: From Molecular Mechanisms to Targeted Therapy. *Signal Transduct. Target. Ther.* **2024**, *9*, 274. [CrossRef]
8. Michailidou, K.; Lindström, S.; Dennis, J.; Beesley, J.; Hui, S.; Kar, S.; Lemaçon, A.; Soucy, P.; Glubb, D.; Rostamianfar, A.; et al. Association Analysis Identifies 65 New Breast Cancer Risk Loci. *Nature* **2017**, *551*, 92–94. [CrossRef]
9. Phelan, C.M.; Kuchenbaecker, K.B.; Tyrer, J.P.; Kar, S.P.; Lawrenson, K.; Winham, S.J.; Dennis, J.; Pirie, A.; Riggan, M.J.; Chornokur, G.; et al. Identification of 12 New Susceptibility Loci for Different Histotypes of Epithelial Ovarian Cancer. *Nat. Genet.* **2017**, *49*, 680–691. [CrossRef]
10. Schumacher, F.R.; Al Olama, A.A.; Berndt, S.I.; Benlloch, S.; Ahmed, M.; Saunders, E.J.; Dadaev, T.; Leongamornlert, D.; Anokian, E.; Cieza-Borrella, C.; et al. Association Analyses of More than 140,000 Men Identify 63 New Prostate Cancer Susceptibility Loci. *Nat. Genet.* **2018**, *50*, 928–936. [CrossRef]
11. O'Mara, T.A.; Glubb, D.M.; Amant, F.; Annibali, D.; Ashton, K.; Attia, J.; Auer, P.L.; Beckmann, M.W.; Black, A.; Bolla, M.K.; et al. Identification of Nine New Susceptibility Loci for Endometrial Cancer. *Nat. Commun.* **2018**, *9*, 3166. [CrossRef] [PubMed]
12. de Lange, K.M.; Moutsianas, L.; Lee, J.C.; Lamb, C.A.; Luo, Y.; Kennedy, N.A.; Jostins, L.; Rice, D.L.; Gutierrez-Achury, J.; Ji, S.-G.; et al. Genome-Wide Association Study Implicates Immune Activation of Multiple Integrin Genes in Inflammatory Bowel Disease. *Nat. Genet.* **2017**, *49*, 256–261. [CrossRef] [PubMed]
13. Okada, Y.; Wu, D.; Trynka, G.; Raj, T.; Terao, C.; Ikari, K.; Kochi, Y.; Ohmura, K.; Suzuki, A.; Yoshida, S.; et al. Genetics of Rheumatoid Arthritis Contributes to Biology and Drug Discovery. *Nature* **2014**, *506*, 376–381. [CrossRef] [PubMed]
14. Bentham, J.; Morris, D.L.; Graham, D.S.C.; Pinder, C.L.; Tombleson, P.; Behrens, T.W.; Martín, J.; Fairfax, B.P.; Knight, J.C.; Chen, L.; et al. Genetic Association Analyses Implicate Aberrant Regulation of Innate and Adaptive Immunity Genes in the Pathogenesis of Systemic Lupus Erythematosus. *Nat. Genet.* **2015**, *47*, 1457–1464. [CrossRef]
15. Saevarsdottir, S.; Olafsdottir, T.A.; Ivarsdottir, E.V.; Halldorsson, G.H.; Gunnarsdottir, K.; Sigurdsson, A.; Johannesson, A.; Sigurdsson, J.K.; Juliusdottir, T.; Lund, S.H.; et al. FLT3 Stop Mutation Increases FLT3 Ligand Level and Risk of Autoimmune Thyroid Disease. *Nature* **2020**, *584*, 619–623. [CrossRef]
16. International Multiple Sclerosis Genetics Consortium (IMSGC); Beecham, A.H.; Patsopoulos, N.A.; Xifara, D.K.; Davis, M.F.; Kemppinen, A.; Cotsapas, C.; Shah, T.S.; Spencer, C.; Booth, D.; et al. Analysis of Immune-Related Loci Identifies 48 New Susceptibility Variants for Multiple Sclerosis. *Nat. Genet.* **2013**, *45*, 1353–1360.
17. Robertson, C.C.; Inshaw, J.R.J.; Onengut-Gumuscu, S.; Chen, W.-M.; Santa Cruz, D.F.; Yang, H.; Cutler, A.J.; Crouch, D.J.M.; Farber, E.; Bridges, S.L.; et al. Fine-Mapping, Trans-Ancestral and Genomic Analyses Identify Causal Variants, Cells, Genes and Drug Targets for Type 1 Diabetes. *Nat. Genet.* **2021**, *53*, 962–971. [CrossRef]

18. Willer, C.J.; Li, Y.; Abecasis, G.R. METAL: Fast and Efficient Meta-Analysis of Genomewide Association Scans. *Bioinformatics* **2010**, *26*, 2190–2191. [CrossRef]
19. Kar, S.P.; Beesley, J.; Amin Al Olama, A.; Michailidou, K.; Tyrer, J.; Kote-Jarai, Z.; Lawrenson, K.; Lindstrom, S.; Ramus, S.J.; Thompson, D.J.; et al. Genome-Wide Meta-Analyses of Breast, Ovarian, and Prostate Cancer Association Studies Identify Multiple New Susceptibility Loci Shared by at Least Two Cancer Types. *Cancer Discov.* **2016**, *6*, 1052–1067. [CrossRef]
20. Watanabe, K.; Taskesen, E.; van Bochoven, A.; Posthuma, D. Functional Mapping and Annotation of Genetic Associations with FUMA. *Nat. Commun.* **2017**, *8*, 1826. [CrossRef]
21. Stacey, D.; Fauman, E.B.; Ziemek, D.; Sun, B.B.; Harshfield, E.L.; Wood, A.M.; Butterworth, A.S.; Suhre, K.; Paul, D.S. ProGeM: A Framework for the Prioritization of Candidate Causal Genes at Molecular Quantitative Trait Loci. *Nucleic Acids Res.* **2019**, *47*, e3. [CrossRef] [PubMed]
22. Chaussabel, D.; Baldwin, N. Democratizing Systems Immunology with Modular Transcriptional Repertoire Analyses. *Nat. Rev. Immunol.* **2014**, *14*, 271–280. [CrossRef]
23. Li, S.; Rouphael, N.; Duraisingham, S.; Romero-Steiner, S.; Presnell, S.; Davis, C.; Schmidt, D.S.; Johnson, S.E.; Milton, A.; Rajam, G.; et al. Molecular Signatures of Antibody Responses Derived from a Systems Biology Study of Five Human Vaccines. *Nat. Immunol.* **2014**, *15*, 195–204. [CrossRef] [PubMed]
24. Kuleshov, M.V.; Jones, M.R.; Rouillard, A.D.; Fernandez, N.F.; Duan, Q.; Wang, Z.; Koplev, S.; Jenkins, S.L.; Jagodnik, K.M.; Lachmann, A.; et al. Enrichr: A Comprehensive Gene Set Enrichment Analysis Web Server 2016 Update. *Nucleic Acids Res.* **2016**, *44*, W90–W97. [CrossRef]
25. Cerami, E.; Gao, J.; Dogrusoz, U.; Gross, B.E.; Sumer, S.O.; Aksoy, B.A.; Jacobsen, A.; Byrne, C.J.; Heuer, M.L.; Larsson, E.; et al. The cBio Cancer Genomics Portal: An Open Platform for Exploring Multidimensional Cancer Genomics Data. *Cancer Discov.* **2012**, *2*, 401–404. [CrossRef]
26. Han, Y.; Wang, Y.; Dong, X.; Sun, D.; Liu, Z.; Yue, J.; Wang, H.; Li, T.; Wang, C. TISCH2: Expanded Datasets and New Tools for Single-Cell Transcriptome Analyses of the Tumor Microenvironment. *Nucleic Acids Res.* **2023**, *51*, D1425–D1431. [CrossRef]
27. Ghoussaini, M.; Mountjoy, E.; Carmona, M.; Peat, G.; Schmidt, E.M.; Hercules, A.; Fumis, L.; Miranda, A.; Carvalho-Silva, D.; Buniello, A.; et al. Open Targets Genetics: Systematic Identification of Trait-Associated Genes Using Large-Scale Genetics and Functional Genomics. *Nucleic Acids Res.* **2021**, *49*, D1311–D1320. [CrossRef]
28. Võsa, U.; Claringbould, A.; Westra, H.-J.; Bonder, M.J.; Deelen, P.; Zeng, B.; Kirsten, H.; Saha, A.; Kreuzhuber, R.; Yazar, S.; et al. Large-Scale Cis- and Trans-eQTL Analyses Identify Thousands of Genetic Loci and Polygenic Scores That Regulate Blood Gene Expression. *Nat. Genet.* **2021**, *53*, 1300–1310. [CrossRef]
29. GTEx Consortium. The GTEx Consortium Atlas of Genetic Regulatory Effects across Human Tissues. *Science* **2020**, *369*, 1318–1330. [CrossRef]
30. Dong, S.; Zhao, N.; Spragins, E.; Kagda, M.S.; Li, M.; Assis, P.; Jolanki, O.; Luo, Y.; Cherry, J.M.; Boyle, A.P.; et al. Annotating and Prioritizing Human Non-Coding Variants with RegulomeDB v.2. *Nat. Genet.* **2023**, *55*, 724–726. [CrossRef]
31. Raies, A.; Tulodziecka, E.; Stainer, J.; Middleton, L.; Dhindsa, R.S.; Hill, P.; Engkvist, O.; Harper, A.R.; Petrovski, S.; Vitsios, D. DrugnomeAI Is an Ensemble Machine-Learning Framework for Predicting Druggability of Candidate Drug Targets. *Commun. Biol.* **2022**, *5*, 1291. [CrossRef] [PubMed]
32. Shao, L.; Hou, W.; Scharping, N.E.; Vendetti, F.P.; Srivastava, R.; Roy, C.N.; Menk, A.V.; Wang, Y.; Chauvin, J.-M.; Karukonda, P.; et al. IRF1 Inhibits Antitumor Immunity through the Upregulation of PD-L1 in the Tumor Cell. *Cancer Immunol. Res.* **2019**, *7*, 1258–1266. [CrossRef] [PubMed]
33. Yan, Y.; Zheng, L.; Du, Q.; Yan, B.; Geller, D.A. Interferon Regulatory Factor 1 (IRF-1) and IRF-2 Regulate PD-L1 Expression in Hepatocellular Carcinoma (HCC) Cells. *Cancer Immunol. Immunother.* **2020**, *69*, 1891–1903. [CrossRef]
34. Wu, Y.; Zhou, L.; Zou, Y.; Zhang, Y.; Zhang, M.; Xu, L.; Zheng, L.; He, W.; Yu, K.; Li, T.; et al. Disrupting the Phase Separation of KAT8-IRF1 Diminishes PD-L1 Expression and Promotes Antitumor Immunity. *Nat. Cancer* **2023**, *4*, 382–400. [CrossRef]
35. Payne, K.J.; Dovat, S. Ikaros and Tumor Suppression in Acute Lymphoblastic Leukemia. *Crit. Rev. Oncog.* **2011**, *16*, 3–12. [CrossRef]
36. Chen, J.C.; Perez-Lorenzo, R.; Saenger, Y.M.; Drake, C.G.; Christiano, A.M. IKZF1 Enhances Immune Infiltrate Recruitment in Solid Tumors and Susceptibility to Immunotherapy. *Cell Syst.* **2018**, *7*, 92–103.e4. [CrossRef]
37. Feng, H.; Wang, T.; Ye, J.; Yang, Y.; Huang, X.; Lai, D.; Lv, Z.; Huang, Y.; Zhang, X. SPI1 Is a Prognostic Biomarker of Immune Infiltration and Immunotherapy Efficacy in Clear Cell Renal Cell Carcinoma. *Discov. Oncol.* **2022**, *13*, 134. [CrossRef]
38. Luo, Q.; Dong, Z.; Xie, W.; Fu, X.; Lin, L.; Zeng, Q.; Chen, Y.; Ye, G.; Chen, M.; Hu, H.; et al. Apatinib Remodels the Immunosuppressive Tumor Ecosystem of Gastric Cancer Enhancing Anti-PD-1 Immunotherapy. *Cell Rep.* **2023**, *42*, 112437. [CrossRef]
39. Willman, C.L. SH2B3: A New Leukemia Predisposition Gene. *Blood* **2013**, *122*, 2293–2295. [CrossRef]

40. Wang, L.-N.; Zhang, Z.-T.; Wang, L.; Wei, H.-X.; Zhang, T.; Zhang, L.-M.; Lin, H.; Zhang, H.; Wang, S.-Q. TGF-B1/SH2B3 Axis Regulates Anoikis Resistance and EMT of Lung Cancer Cells by Modulating JAK2/STAT3 and SHP2/Grb2 Signaling Pathways. *Cell Death Dis.* **2022**, *13*, 472. [CrossRef]
41. Katayama, H.; Mori, T.; Seki, Y.; Anraku, M.; Iseki, M.; Ikutani, M.; Iwasaki, Y.; Yoshida, N.; Takatsu, K.; Takaki, S. Lnk Prevents Inflammatory $CD8^+$ T-Cell Proliferation and Contributes to Intestinal Homeostasis. *Eur. J. Immunol.* **2014**, *44*, 1622–1632. [CrossRef]
42. Pant, T.; Foda, B.; Geurts, A.; Chen, Y.-G. Lnk/Sh2b3 Modulates Bioenergetic Metabolism of Activated CD8 T Cells and Control the Development of Type 1 Diabetes. *J. Immunol.* **2023**, *210*, 77.03. [CrossRef]
43. Kuo, C.-L.; Joaquim, M.; Kuchel, G.A.; Ferrucci, L.; Harries, L.W.; Pilling, L.C.; Melzer, D. The Longevity-Associated SH2B3 (LNK) Genetic Variant: Selected Aging Phenotypes in 379,758 Subjects. *J. Gerontol. A Biol. Sci. Med. Sci.* **2020**, *75*, 1656–1662. [CrossRef] [PubMed]
44. Turker, I.; Sharma, A.; Huang, S.; Johnson, D.B.; Alexander, M.R. Combination Immune Checkpoint Inhibitor Therapy Is Associated With Increased Blood Pressure in Melanoma Patients. *Hypertension* **2023**, *80*, e43–e45. [CrossRef] [PubMed]
45. Lo, W.-L.; Shah, N.H.; Rubin, S.A.; Zhang, W.; Horkova, V.; Fallahee, I.R.; Stepanek, O.; Zon, L.I.; Kuriyan, J.; Weiss, A. Slow Phosphorylation of a Tyrosine Residue in LAT Optimizes T Cell Ligand Discrimination. *Nat. Immunol.* **2019**, *20*, 1481–1493. [CrossRef]
46. Balagopalan, L.; Ashwell, B.A.; Bernot, K.M.; Akpan, I.O.; Quasba, N.; Barr, V.A.; Samelson, L.E. Enhanced T-Cell Signaling in Cells Bearing Linker for Activation of T-Cell (LAT) Molecules Resistant to Ubiquitylation. *Proc. Natl. Acad. Sci. USA* **2011**, *108*, 2885–2890. [CrossRef]
47. Kent, A.; Longino, N.V.; Christians, A.; Davila, E. Naturally Occurring Genetic Alterations in Proximal TCR Signaling and Implications for Cancer Immunotherapy. *Front. Immunol.* **2021**, *12*, 658611. [CrossRef]
48. Charlton, B.; Lafferty, K.J. The Th1/Th2 Balance in Autoimmunity. *Curr. Opin. Immunol.* **1995**, *7*, 793–798. [CrossRef]
49. Knutson, K.L.; Disis, M.L. Tumor Antigen-Specific T Helper Cells in Cancer Immunity and Immunotherapy. *Cancer Immunol. Immunother.* **2005**, *54*, 721–728. [CrossRef]
50. Ellyard, J.I.; Simson, L.; Parish, C.R. Th2-Mediated Anti-Tumour Immunity: Friend or Foe? *Tissue Antigens* **2007**, *70*, 1–11. [CrossRef]
51. Wei, S.C.; Duffy, C.R.; Allison, J.P. Fundamental Mechanisms of Immune Checkpoint Blockade Therapy. *Cancer Discov.* **2018**, *8*, 1069–1086. [CrossRef] [PubMed]
52. Ozga, A.J.; Chow, M.T.; Luster, A.D. Chemokines and the Immune Response to Cancer. *Immunity* **2021**, *54*, 859–874. [CrossRef] [PubMed]
53. Hollande, C.; Boussier, J.; Ziai, J.; Nozawa, T.; Bondet, V.; Phung, W.; Lu, B.; Duffy, D.; Paradis, V.; Mallet, V.; et al. Inhibition of the Dipeptidyl Peptidase DPP4 (CD26) Reveals IL-33-Dependent Eosinophil-Mediated Control of Tumor Growth. *Nat. Immunol.* **2019**, *20*, 257–264. [CrossRef] [PubMed]
54. Fatumo, S.; Chikowore, T.; Choudhury, A.; Ayub, M.; Martin, A.R.; Kuchenbaecker, K. A Roadmap to Increase Diversity in Genomic Studies. *Nat. Med.* **2022**, *28*, 243–250. [CrossRef]
55. Groha, S.; Alaiwi, S.A.; Xu, W.; Naranbhai, V.; Nassar, A.H.; Bakouny, Z.; El Zarif, T.; Saliby, R.M.; Wan, G.; Rajeh, A.; et al. Germline Variants Associated with Toxicity to Immune Checkpoint Blockade. *Nat. Med.* **2022**, *28*, 2584–2591. [CrossRef]
56. Kinnersley, B.; Sud, A.; Coker, E.A.; Tym, J.E.; Di Micco, P.; Al-Lazikani, B.; Houlston, R.S. Leveraging Human Genetics to Guide Cancer Drug Development. *JCO Clin. Cancer Inform.* **2018**, *2*, 1–11. [CrossRef]
57. Minikel, E.V.; Painter, J.L.; Dong, C.C.; Nelson, M.R. Refining the Impact of Genetic Evidence on Clinical Success. *Nature* **2024**, *629*, 624–629. [CrossRef]